AD-A087 677 STANFORD UNIV CA EDWARD L GINZTON LAB F/G 20/1
ACOUSTIC MICROSCOPY AT CRYOGENIC TEMPERATURES.(U)
JUL 80 C F QUATE, J HEISERMAN N00014-77-C-0412
UNCLASSIFIED GL-3149 NL

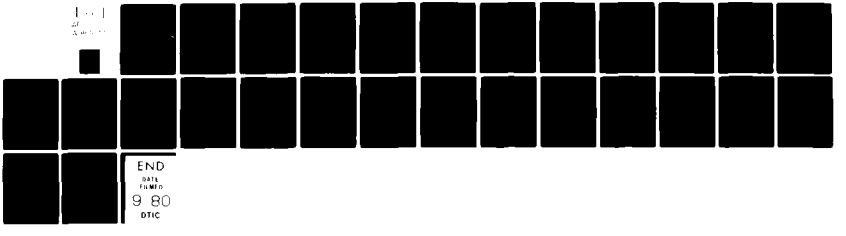

END
DATE FILMED
9 80
DTIC

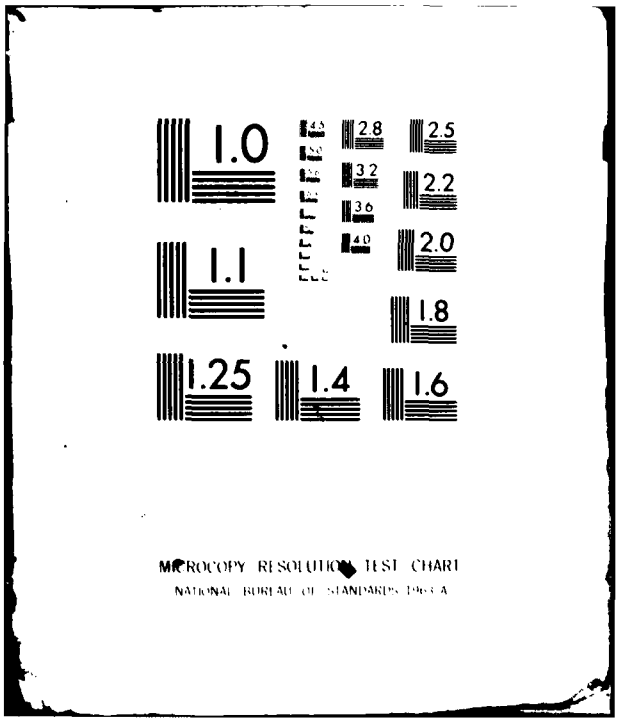
1.0
1.1
1.25
1.4
1.6
1.8
2.0
2.2
2.5
2.8
3.2
3.6
4.0
MICROCOPY RESOLUTION TEST CHART
NATIONAL BUREAU OF STANDARDS 1963-A

ACOUSTIC MICROSCOPY AT CRYOGENIC TEMPERATURES

Annual Summary Report

1 Jul 79 – 30 Jun 80

Contract No. N00014-77-C-0412

G.L. Report No. 3149

Jul 80

Edward L. Ginzton Laboratory
W. W. Hansen Laboratories of Physics
Stanford University
Stanford, California

UNCLASSIFIED

SECURITY CLASSIFICATION OF THIS PAGE (When Data Entered)

REPORT DOCUMENTATION PAGE	READ INSTRUCTIONS BEFORE COMPLETING FORM
1. REPORT NUMBER	2. GOVT ACCESSION NO. AD-A087677 / 3. RECIPIENT'S CATALOG NUMBER
4. TITLE (and Subtitle) ACOUSTIC MICROSCOPY AT CRYOGENIC TEMPERATURES	5. TYPE OF REPORT & PERIOD COVERED Annual Summary Report 1 July 1979 – 30 June 1980
	6. PERFORMING ORG. REPORT NUMBER G.L. Report No. 3149 /
7. AUTHOR(s) C.F. Quate J. Heiserman	8. CONTRACT OR GRANT NUMBER(s) N00014-77-C-0412 /
9. PERFORMING ORGANIZATION NAME AND ADDRESS Edward L. Ginzton Laboratory / W.W. Hansen Laboratories of Physics Stanford University, Stanford, CA 94305	10. PROGRAM ELEMENT, PROJECT, TASK AREA & WORK UNIT NUMBERS Task NR384-924
11. CONTROLLING OFFICE NAME AND ADDRESS Office of Naval Research Physics Program Office Arlington, Virginia 22217	12. REPORT DATE July 1980
	13. NUMBER OF PAGES 26
14. MONITORING AGENCY NAME & ADDRESS(if different from Controlling Office)	15. SECURITY CLASS. (of this report) UNCLASSIFIED
	15a. DECLASSIFICATION/DOWNGRADING SCHEDULE

16. DISTRIBUTION STATEMENT (of this Report)

"Approved for public release; distribution unlimited"

17. DISTRIBUTION STATEMENT (of the abstract entered in Block 20, if different from Report)

18. SUPPLEMENTARY NOTES

19. KEY WORDS (Continue on reverse side if necessary and identify by block number)

Acoustic microscopy	Superfluid helium
Liquid argon	Liquid nitrogen
Mechanical scanning	High frequency acoustic properties

20. ABSTRACT (Continue on reverse side if necessary and identify by block number)

This report summarizes our progress in development of high resolution acoustic microscopes for use at cryogenic temperatures. During the past year we have concentrated on development of efficient acoustic matching layers for use in liquid helium and extension of our techniques to temperatures below 0.5°K in liquid helium. As a first step at these low temperatures, we have begun probing the acoustic properties of the liquid at frequencies at least 5 times higher than previously published results.

DD FORM 1 JAN 73 1473 EDITION OF 1 NOV 65 IS OBSOLETE

UNCLASSIFIED

SECURITY CLASSIFICATION OF THIS PAGE (When Data Entered)

ANNUAL SUMMARY REPORT

ACOUSTIC MICROSCOPY AT CRYOGENIC TEMPERATURES

During the past year we have been working to extend the usefulness of the acoustic microscope in cryogenic liquids and to improve the performance of the instrument, especially in liquid helium. We have also initiated a program to explore the high frequency acoustic properties of superfluid helium below 0.5°K.

I. ACOUSTIC MATCHING LAYERS FOR USE IN SUPERFLUID HELIUM

For the liquid helium acoustic microscope to perform optimally in terms of achievable resolution and signal-to-noise ratio of its imaging, acoustic energy must be transmitted across the sapphire lens-helium interface as efficiently as possible. The major obstacle to efficient power transmission is the large acoustic impedance mismatch between sapphire ($z_S = 44.3 \times 10^5$ gm/cm^2-sec) and helium ($z_{He} = 0.03 \times 10^5$ gm/cm^2-sec). At a sapphire-helium interface only 0.3% of the acoustic power incident in a plane wave will be transmitted.

A standard approach for solving a mismatch problem with coherent waves is to place one or more quarter wavelength matching layers between the solid and the liquid. The ideal matching layer would have an acoustic impedance equal to the geometric mean of the values for the solid and liquid. For sapphire and liquid helium the ideal impedance value is 1.2×10^5 gm/cm^2-sec. Few materials suitable for thin film fabrication have impedance low enough

to be near this value. The range of suitable low impedance materials can be extended by using a double matching layer system and choosing the impedance of the first layer to be very high. This effectively increases the impedance of the lens material and raises the ideal impedance of the second layer.

In a previous report we described the successful fabrication and testing of an acoustic lens incorporating quarter wave matching layers made of gold and glass. Acoustic power transmission from sapphire to helium using this matching layer combination was about 6%. We were able to do acoustic imaging using these matching layers although the signal-to-noise ratio was poor.

During the past year we have worked to improve the transmission characteristics of the matching layers. We have concentrated on two schemes: 1) a single quarter wave layer of low impedance carbon, and 2) a double layer combination of tungsten and carbon. Preliminary test results indicate that both of these schemes will significantly improve acoustic lens performance.

Tungsten and carbon are refractory materials and require high temperatures for evaporation. An electron beam evaporation station has been assembled that is capable of depositing these materials for matching layers. The microstructure of the deposited films is a function of substrate temperature. For this reason, provision has been made for heating the sapphire lens substrate up to 800°C during deposition.

Vitreous carbon disks[1] were found to be a satisfactory source material for E-beam deposition of carbon layers. Graphite[2] was found to be unsuitable because of gases trapped within the material. Vitreous carbon was found to be free of gas. Vitreous carbon is quite brittle and the target material is prone

---

[1] Type D83-1 Vitrecarb disks from Fluorocarbon Process Systems Division, Anaheim, CA.

[2] Grade UF-4S from Ultra Carbon, Bay City, Michigan.

to breaking during the evaporation step due to thermal stresses. The electron beam is scanned in two dimensions so as to heat the carbon target as evenly as possible during evaporation to prevent breakage.

Carbon films deposited directly on sapphire were found to have poor adhesion. Satisfactory adhesion was obtained by including a thin (400 - 1000 Å) tungsten interface layer between the sapphire and carbon. Adhesion of carbon to tungsten is good presumably because tungsten forms a stable carbide.[3] Carbon films deposited on sapphire/tungsten at 750°C are mechanically stable and well adhering, as determined by the "scotch tape" test. They may be cycled repeatedly from room temperature to cryogenic temperatures without apparent degradation of adhesion. To the eye, the carbon films appear black and are good specular reflectors. Microscopic examination reveals that some submicron surface structure is present. Control of this structure is still being investigated. Its effect on the imaging properties of a carbon coated lens is not yet known.

The acoustic properties of a quarter wave layer of carbon on sapphire have been investigated in liquid helium at 4.2°K. Carbon films were deposited on sapphire "flats" and excited with plane waves. Using the pulse-echo method, the power reflection coefficient R was measured as a function of frequency in the neighborhood of the resonant frequency f_o. The carbon layer was assumed to be lossless and the transmission $T(f)$ into helium was calculated according to $T(f) = 1 - R(f)$. Figure 1 shows measurements $T(f)$ for a carbon film with center frequency of 960 MHz. At the center frequency approximately 30% of the incident acoustic power is transmitted into the liquid. The 3 dB

---

[3] W.H. Smith and D.H. Leeds in Modern Materials (Academic, New York, 1970), Vol. 7.

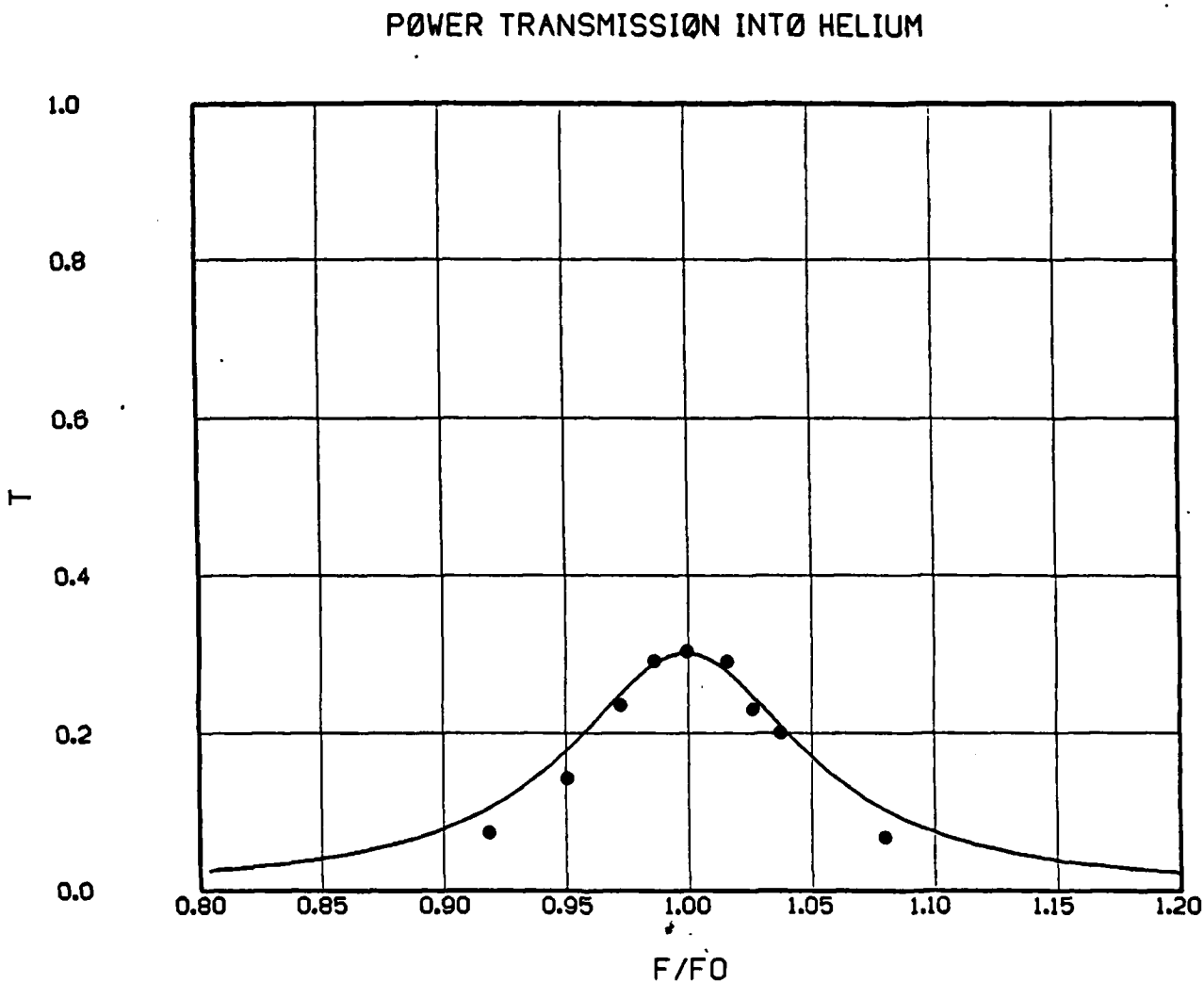

FIG. 1--Acoustic power transmission from sapphire to liquid helium for a single quarter wavelength carbon matching layer. The solid line is the theoretical response based on $Z_c = 4.0 \times 10^5$ gm/cm^2-sec. The points are experimental.

bandwidth for transmission is observed to be about 13%.

In terms of acoustic impedances, transmission of a plane wave into liquid helium at the center frequency is given by

$$T(f_o) = \frac{4\, Z_{He}\, Z_c^2/Z_S}{(Z_{He} + Z_c^2/Z_S)^2}$$

where

Z_{He} = Helium impedance = 0.03×10^5 gm/cm^2-sec

Z_S = Sapphire impedance = 44.3×10^5 gm/cm^2-sec

Z_c = Carbon impedance.

By inverting the above equation and using the experimental value $T(f_o) = 0.30$, the acoustic impedance of the carbon film was determined to be 4.0×10^5 gm/cm^2-sec. The solid line in Fig. 1 shows the theoretical transmission into helium as a function of frequency based on this value of carbon impedance.

A two-layer impedance matching system consisting of a quarter wave layer of tungsten on sapphire followed by a quarter wave layer of carbon further improves the power transmission into helium. Tungsten is a good choice for the first layer because of its very high impedance ($Z_w = 105 \times 10^5$ gm/cm^2-sec). The tungsten layer effectively increases the impedance of the lens material so that the ideal impedance for the low impedance second layer is 2.7×10^5 gm/cm^2-sec. This is more than twice the ideal impedance of the layer in the single layer system.

Tungsten films 1.6 μm in thickness (quarter wave at 750 MHz) deposited directly onto a 600°C sapphire substrate were found to be inadequately adhered to the substrate. Films deposited at 750°C were found to be smooth, well adhering and mechanically stable. Further improvement in adhesion of the

tungsten films was obtained when a 150 Å titanium interface layer was included between the substrate and the tungsten film. This improvement was expected since titanium adheres well to sapphire and is partially soluble in tungsten at temperatures above 600°C.[4] At the present time smooth and well-adhering tungsten films as thick as 2 μm can be routinely fabricated. The films can be cycled repeatedly between room temperature and cryogenic temperatures without apparent degradation.

The acoustic properties of a tungsten-carbon matching layer combination were investigated in liquid helium at 4.2°K. The tungsten-carbon layers were fabricated on sapphire flats and excited with plane waves. The method for determining transmission as a function of frequency, $T(f)$, was similar to that described for the single carbon layer. Figure 2 shows measured values of $T(f)$ for tungsten-carbon matching layers. The center frequency, f_o, was 680 MHz. At the center frequency approximately 82% of the incident acoustic power is transmitted into the helium. The 3 dB bandwidth is approximately 3%. The solid line in Fig. 2 shows the theoretical transmission into helium based on $Z_w = 105 \times 10^5$ gm/cm^2-sec and $Z_c = 4.2 \times 10^5$ gm/cm^2-sec.

In summary we have successfully fabricated well-adhering thin films of tungsten and carbon by E-beam evaporation. The carbon films were found to have a very low value of acoustic impedance, approximately 4×10^5 g/cm^2-sec. Power transmission into helium for a single carbon layer on sapphire was found to be 30%. With the two layer system of tungsten and carbon, transmission improved to 82%. This is a significant improvement over the 6%

---

[4] J.A. Cunningham, C.R. Fuller, and C.T. Haywood, IEEE Trans. on Reliability R-19, 182 (1970).

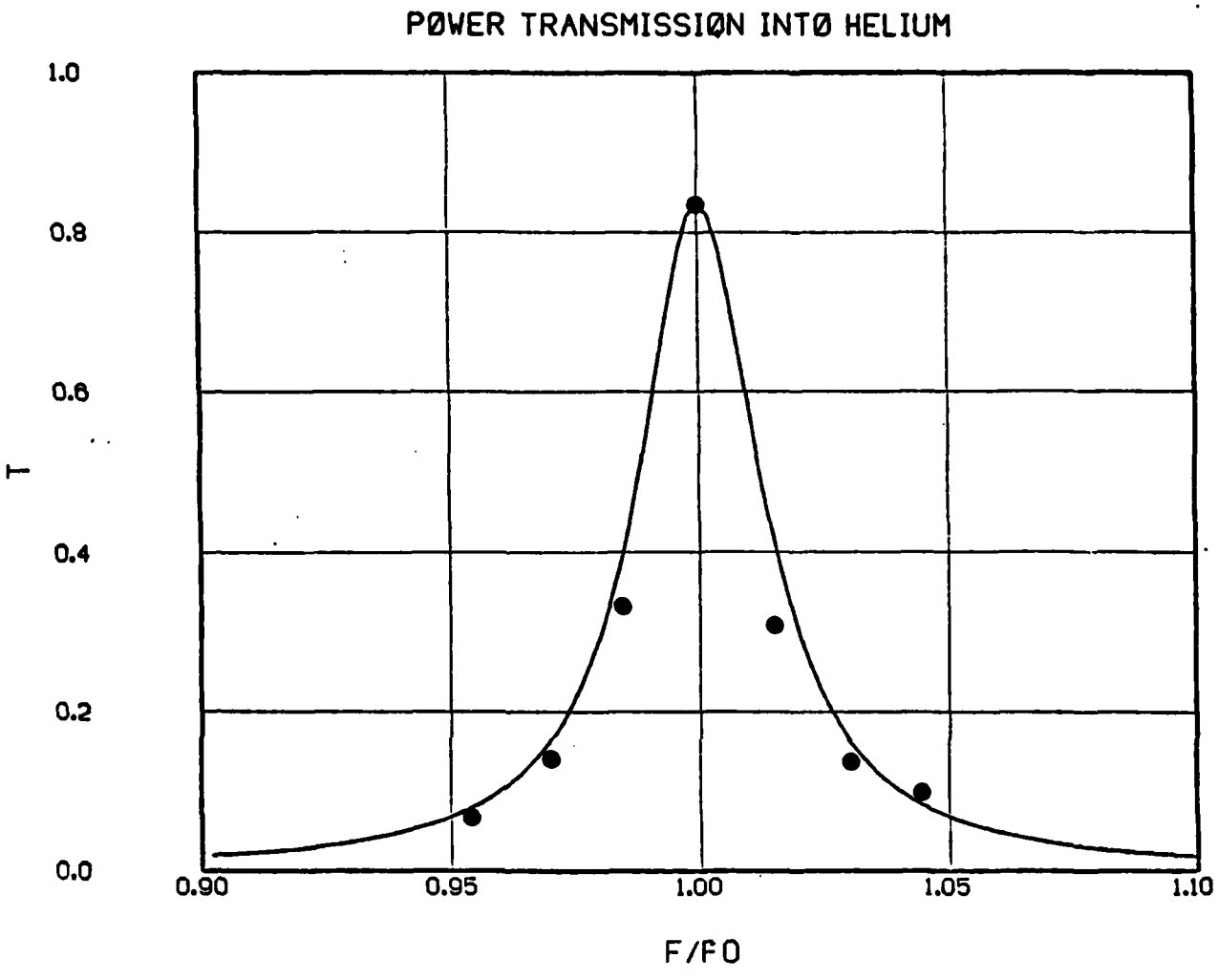

FIG. 2--Acoustic power transmission from sapphire to liquid helium for tungsten-carbon quarter wave matching layers. The solid line is the theoretical response based on $Z_c = 4.2 \times 10^5$ gm/cm^2-sec and $Z_w = 105 \times 10^5$ gm/cm^2-sec . The points are experimental.

transmission achieved previously with gold-glass matching layers. Acoustic lenses for use in superfluid helium at 1.95°K will soon be tested with either carbon or tungsten-carbon matching layers.

II. OPERATION AT TEMPERATURES BELOW 0.5°K

In order to take advantage of the favorable conditions for acoustic microscopy found in superfluid helium below 0.5°K, we have acquired and installed a dilution refrigerator system capable of reaching temperatures down to about 15×10^{-3}°K (15 mK). The system was supplied with a top loading chamber and an experimental access tube which allows us to rapidly exchange an experimental apparatus or sample. The refrigerator is shown schematically in Fig. 3. Typically a small sample can be inserted and cooled to about 100 mK in one hour. We have also cooled a relatively large experimental apparatus to 200 mK in liquid helium in less than two hours. The usefulness of the top loader was proven when it was necessary to remove an experiment to repair a broken lead. This was accomplished in a few hours instead of the several days required to warm and recool the entire refrigerator.

Because of the rather unusual conditions under which we operate our machine, two novel aspects have come to light.

(a) Thermal Grounding of Microwave Coaxial Line

Because of the very high frequencies we employ (we presently work at 1 GHz and expect eventually to operate between 5 and 10 GHz) it is necessary to have a well matched low loss microwave transmission line extending from room temperature to our experimental cell. At the same time, it is necessary to minimize heat transport to avoid exceeding the cooling capacity of the

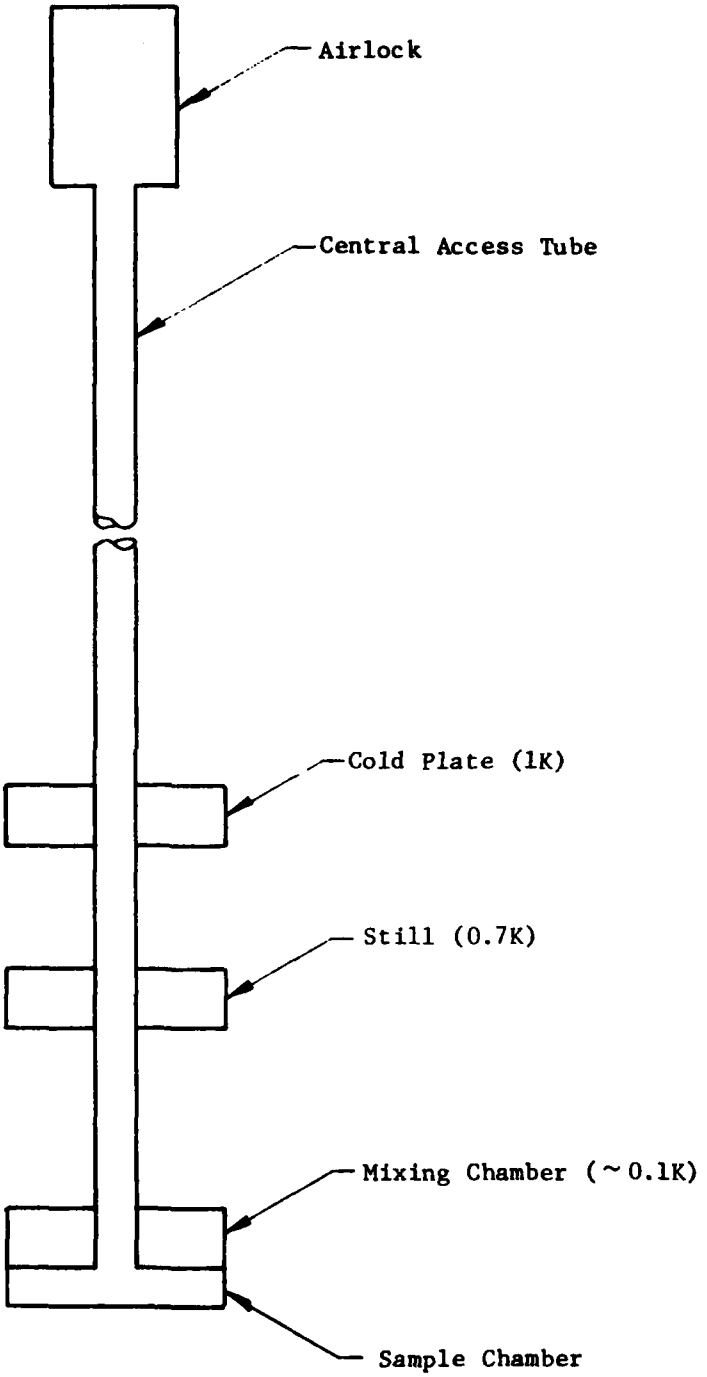

FIG. 3--Schematic of the dilution refrigerator with sample changer.

refrigerator. Conventional stainless steel semirigid coaxial cable[5] provides an adequate transmission line for our frequencies but allows excessive heat transport. It is possible to thermally ground the outer conductor at appropriate locations on the refrigerator but the inner conductor is more difficult to ground because of the teflon dielectric. If the cable is broken to thermally ground the inner conductor care must be taken to avoid an electrical impedance mismatch. However, by interrupting the coaxial line by a short section of microstrip transmission line, it is possible to provide excellent thermal grounding of both inner and outer conductors while maintaining the electrical line impedance nearly constant.

Microstrip transmission lines were introduced in the early fifties and are widely used in miniature microwave devices.[6] The appropriate geometry is indicated in Fig. 4(a). For the practical case of noninfinite conductor and dielectric widths, closed form analysis is not possible. Several authors have treated various approximate cases; the classic analysis is due to Wheeler.[7] Useful design calculations have also been published.[7,8,9] In order to optimize thermal grounding of the thin conductor we choose a sapphire dielectric. Sapphire combines excellent thermal conductivity (better than brass in the range 1K - 0.5K) with excellent electrical properties ($\varepsilon_r \sim 10$ nearly independent of temperature, negligible loss tangent). Thus the microstrip

---

[5] Uniform Tubes, Inc., Collegeville, PA 19426.

[6] S. March, Microwaves 8, 59(1969), 9, 53 (1970).

[7] H. Wheeler, Trans. Inst. Elect. Electron. Engrs., Microwave Theory and Techniques 12, 280 (1964), 13, 172 (1965).

[8] P. Grivet, The Physics of Transmission Lines at High and Very High Frequencies (Academic Press, New York, 1970), Vol. 1.

[9] C. Smith and R. Chang, IEEE Trans. on Microwave Theory and Techniques MTT-28, 90 (1980).

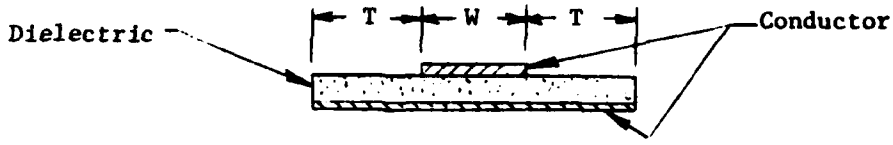

(a)

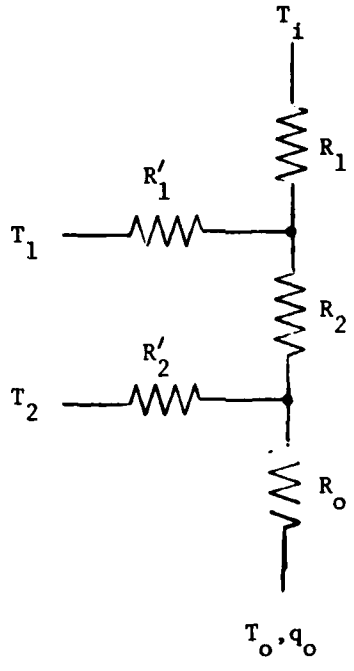

(b)

FIG. 4--(a) Geometry of the microstrip section.
(b) Discrete element thermal model for the microwave transmission line.

section can be attached to an appropriate thermal anchor on the refrigerator and provide a thermal short while maintaining electrical line impedance. For our application we constructed a line consisting of three coaxial sections and two microstrip sections. Dimensions of the various sections are indicated in Table I and Fig. 5. A 50-ohm line impedance was chosen. Room temperature tests using a network analyzer at 1 GHz confirmed that the composite line had a characteristic impedance of about 48 ohms.

Some insight into the operation of the line can be gained by applying a discrete element analysis to derive an expression for the heat load given appropriate thermal anchor temperatures. Consider the network of Fig. 4(b). The ends are held at temperatures T_i and T_o. The thermal resistances (R) are related to thermal conductivities (κ) through the cross sectional area (A) and length of the section (ℓ),

$$R = \frac{\ell}{A\kappa} \tag{1}$$

Figure 4(b) can be analyzed as an "L" section followed by a "T" section. We can assume the primed resistances are much smaller than unprimed. The result is an expression for the heat load q_o:

$$q_o = T_i \frac{R_1' R_2'}{R_o R_1 R_2} + T_1 \frac{R_1' R_2'}{R_o R_1 R_2} + \frac{(T_2 - T_o)}{R_o} \tag{2}$$

To take a realistic example, assume T_i = 1K (cold plate), T_2 - 0.7K (still) and T_o = 100 mK (mixing chamber). R_1 represents a 0.80 m length of .085" diameter stainless steel coax. The geometry is illustrated in Fig. 5. The first 0.60 m is assumed to be in a linear temperature gradient from 4.2K to

TABLE I

Dimensions of Coaxial Line Components

Stainless Steel Coaxial Sections[5]

Type	O.D.	Outer Conductor Cross Sectional Area (m^2)	Inner Conductor Cross Sectional Area (m^2)
UT-85SS	0.086	1.58×10^{-6}	2.23×10^{-7}
UT-205SS	0.020	8.87×10^{-8}	1.27×10^{-8}

Microstrip Line Sections

Type	Material	Width (cm)	Length (cm)	Thickness (cm)
Upper conductor	gold	0.046	2.54	3×10^{-4}
Dielectric	sapphire	0.76	2.54	0.051
Ground Plane	gold	0.76	2.54	3×10^{-4}

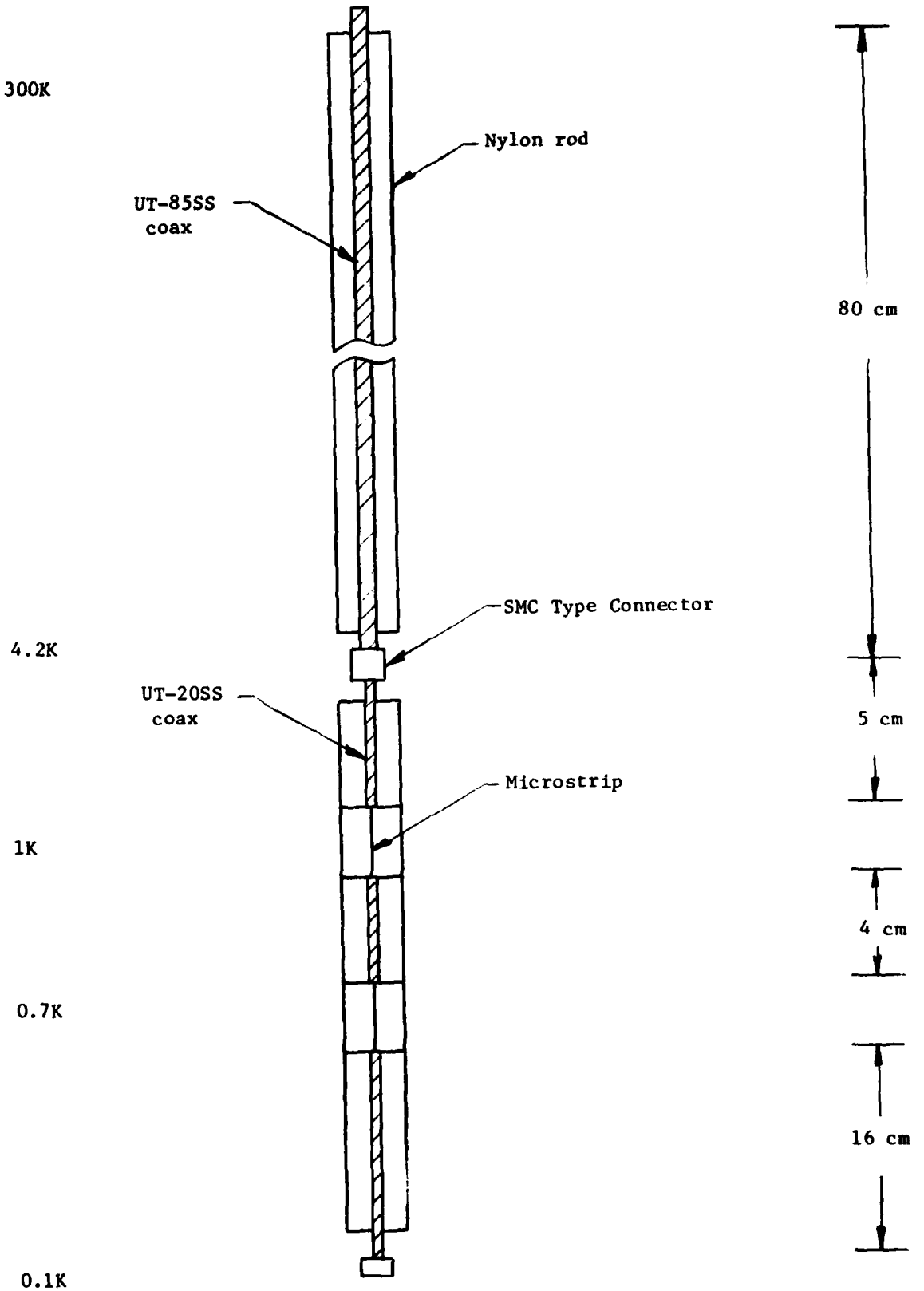

FIG. 5--Schematic of the insertion rod with microwave transmission line.

to 300K. To obtain the average thermal conductivity we approximate the temperature dependence of the thermal conductivity of stainless steel between 1K and 300K by two linear regions as shown in Fig. 6. The average thermal conductivity is given by

$$\bar{\kappa} = \frac{1}{\Delta T} \int_{T_1}^{T_2} \kappa(T) dT \qquad (3)$$

Using (3) and data from Table I and Fig. 6 gives $R = 36.7 \times 10^{-3} \equiv 3.67$ R.U. for the first 0.8m. The next 0.20m of 0.085" diameter coax is held at 4.2K and contributes 44.4 R.U. The next 0.05m is 0.020" diameter coax (UT20-SS) in a gradient between 4.2 and 1K and contributes 383 R.U. Thus $R_1 = 449$ R.U. The series resistance R_2 is composed of 0.4 cm of 0.020" diameter coax between 1 and 0.7°K. Between 1°K and 0.1°K we can approximate the thermal conductivity of stainless steel by[10]

$$K = 0.146T \text{ W/mK} \qquad (4)$$

Using (3) and (4) and then (1) gives $R_2 = 3{,}190$ R.U. Finally R_o is a 0.16m length of 0.020" diameter coax between 0.7K and 0.1K. Thus $R_o = 27{,}100$ R.U.

The shunt resistances all represent heat flow through the sapphire dielectric from the upper conductor. Below 1K the thermal conductivity of sapphire can be approximated by[10]

$$K = 2.67T^3 \text{ W/mK} \qquad (5)$$

---

[10] O. Lounasmaa, Experimental Principles and Methods Below 1K (Academic Press, New York, 1974).

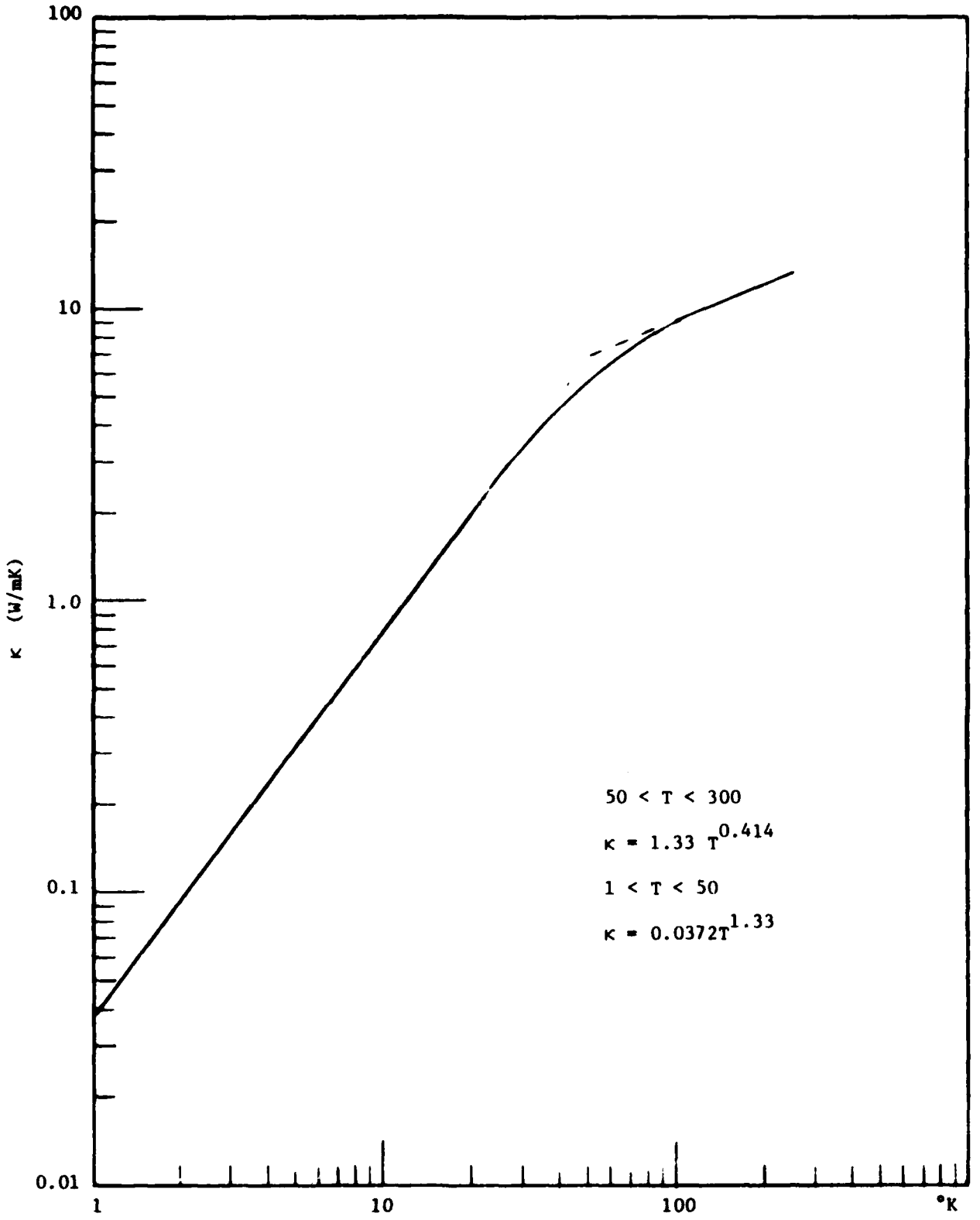

FIG. 6--Thermal conductivity of stainless steel.

As a width we take the conductor linewidth (5×10^{-4} m). Then the two shunt resistances are easily calculated from the data of Table I. The results are $R_1' = 15 \times 10^{-3}$ R.U., $R_2' = 43 \times 10^{-3}$ R.U. All of these values are tabulated in Table II. Using the calculated resistances and the anchor temperatures the heat load can be calculated from (2) and turns out to be 22×10^{-9} W (22 nW). We have neglected the series resistance of the microstrip. Inspection of (2) and Table II reveals that the principal contribution to the load comes from the last term of (2). Thus to improve the operation of the line, the resistance R_o should be increased. It is probably not desirable to reduce the dimensions of the coax at this point but some improvement may be gained by choosing a superconducting coax of appropriate material.

For our application we designed and built a line as described above, imbedded in rods of Nylon for the section above the cold plate and Vespel SP-22,[11] for the section from the cold plate to the experimental chamber just below the mixing chamber. Thermal contact was made to the walls of the access tube by phosphor bronze leaf springs. Although this method of thermal anchoring was surely imperfect, the apparatus was adequate for reaching a sample chamber temperature of 40 mK without helium and 200 mK with helium as described later. An upper limit of 1 μW was established for the heat leak due to the coaxial line.

(b) Film Flow

Because the entire dilution refrigerator (below the cold plate) is held at temperatures below the superfluid transition, a superfluid film can be

[11] E.I. Dupont De Nemoms and Co., Wilmington, DE 19868.

TABLE II

Thermal Resistance Values

$1 \text{ R.U.} = 10^{-3} \text{ K/W}$

	Value (R.U.)
R_1	449
R_2	3190
R_o	27,100
R'_1	15×10^{-3}
R'_2	43×10^{-3}

expected to form when ^4He is condensed in the experimental chamber. This film will extend up the central access tube and because of the unique properties of the superfluid film, may cause a thermal short between the relatively warm still and cold plate and the colder mixing chamber. The mechanism of action of this effect depends on the fact that the superfluid film flows without friction carrying the entropyless superfluid toward the warmer parts of the refrigerator. The liquid helium can then evaporate and the gas can flow back down to the colder areas, reliquify and cause warming. One approach to preventing this is to minimize the open cross section of the central tube to reduce gas backflow. For this reason we have made our probe to closely fit the central tube. It is also possible to add small amounts of ^3He to the superfluid. A certain amount will be adsorbed on the walls of the tube and act as a temperature independent normal fraction, reducing the mass flow of the film. It appears the added helium also reduces the critical velocity of film flow.[12,13]

On the initial run of the refrigerator with helium in the sample chamber, we started with pure ^4He and noted that cooling power was severely degraded, particularly with the sound probe in place. We now believe that much of this is due to faults in the geometry of the sound probe, but at the time in order to continue we added small amounts of ^3He. It was found that about 0.7% ^3He was sufficient to stabilize the refrigerator and allow cooling to about 0.4°K. Increasing the ^3He fraction to 2% allowed cooling to 0.2°K, a temperature sufficiently low for us to carry out our initial investigations.

---

[12] J. Wilks, The Properties of Liquid and Solid Helium (Clarendon Press, Oxford, 1967).

[13] D. Crum, D. Edwards, and R. Sarwinski, Phys. Rev. A 9, 1312 (1974).

We now believe that operation in pure ^{4}He below 0.2°K will be possible after some minor modifications of the acoustic probe, although operation in a 2% solution will allow lower ultimate temperatures to be reached.

III. INITIAL SOUND EXPERIMENT

Because our operating frequencies exceed by at least a factor of five published data at these temperature, we have designed a simple sound cell to perform a series of measurements to determine acoustic attenuation as a function of temperature and frequency. At our frequencies the acoustic wavelength is less than 2000 Å, hence a conventional plane wave experiment is difficult due to the necessity of accurately aligning two plane surfaces. Because of the phase sensitive nature of acoustic transducers, misalignment at the edge of the transducer should be held to less than one-quarter wavelength — less than 500 Å in our case. This alignment problem can be avoided by using an acoustic lens. The lens converts an incident plane wave to a spherical wave converging on a point. If a reflector is placed at the focus, the same lens can be used to collect the reflected acoustic power which is then detected by a transducer, usually the same transducer used to generate the input pulse. All of this is quite familiar to us and is, of course, used in the reflection acoustic microscope. With a fully detailed knowledge of the illumination pattern, aperture, impedance ratio, focal length and any possible apodization due to matching layers, etc., it is possible to determine the absolute values of the acoustic attenuation in a two focal length path and also the acoustic velocity using an acoustic lens. However, for our purposes, just a relative number for the temperature dependence of attenuation is sufficient.

This can be normalized at high temperature to obtain absolute numbers. Bearing in mind the spherical nature of the wavefront in the helium, it is easy to see why an acoustic lens is not sensitive to reflector angle. Rotating the reflector about the focus does not affect the phase-front match at the transducer as is the case for a purely plane wave geometry. The rotated spherical wavefronts still match at the lens surface. Only a small reduction in power occurs because some of the reflected power now misses the lens aperture.

An acoustic lens is ideally suited to relative measurements of attenuation in liquid helium at very low temperatures. The velocity of sound is independent of temperature at low temperatures; this implies that the focal length of the lens is also independent of temperature and so no adjustments need to be made to the focal position while taking data. In addition, the attenuation in the helium is low so the relatively long path lengths required when using a lens are not a disadvantage. In making these measurements we have taken advantage of the top loading feature of our refrigerator and made an experimental apparatus which can be inserted into the central access tube. The coaxial line was described in Section II. The attenuation cell itself is shown in Fig. 7. A sapphire reflector is mounted on a small pedestal and spring loaded into the cell. Adjustable stops limit the total travel to about 0.1 mm and prevent the reflector from touching the lens. When the cell is lowered to the bottom of the sample cell, the pedestal touches and moves the reflector towards the lens. The movement is controlled by a micrometer at the room temperature end of the rod.

In our first attempt we fitted a 1 GHz 100 μm radius lens with a single glass matching layer. The apparatus was cooled to 0.2K. The single matching layer recovered about 25 of the 55 dB two-way loss normally suffered at a

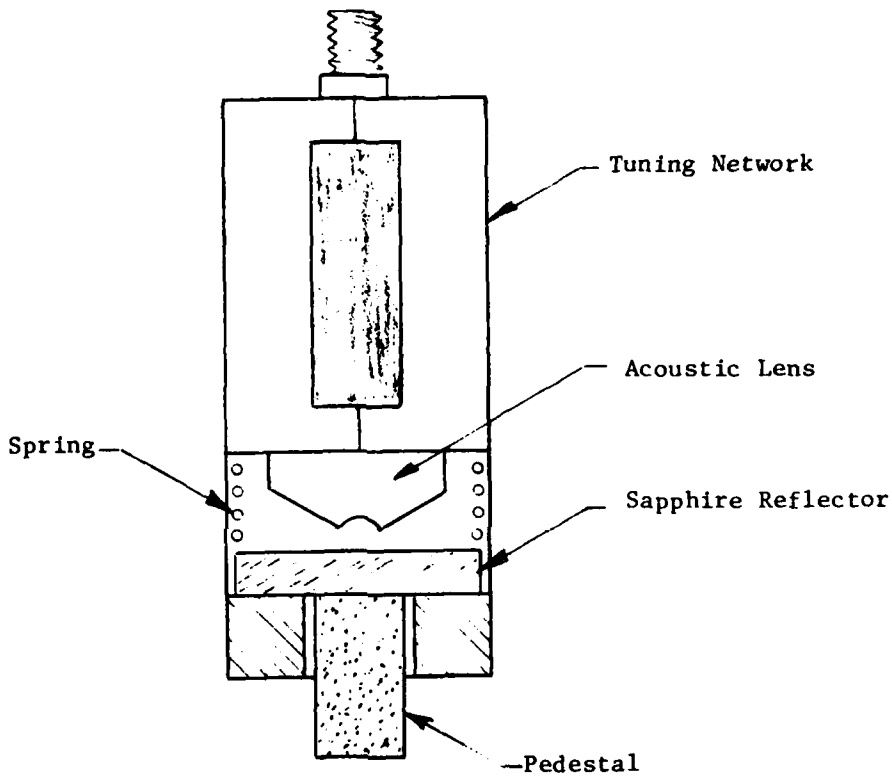

FIG. 7--Schematic of the acoustic attenuation cell.

sapphire-helium interface. For reasons discussed in Section II(b), we used a solution of ^{4}He - 2% ^{3}He as a working liquid. It is possible using a phonon analysis plus a ^{3}He quasiparticle analysis based on the theory of helium solutions proposed by Bardeen, Baym and Pines (BBP)[14,15] to evaluate the expected attenuation in the solution. The contribution of each mechanism is shown in Fig. 8. Also plotted for comparison is the attenuation of room temperature water. The phonon part exhibits the well known T^4 dependence expected in the ballistic limit. The BBP contribution arises from ^{3}He - ^{3}He quasiparticle scattering and shows a resonance near the fermi temperature. At very low temperatures the process is frequency independent and exhibits a T^2 temperature dependence. From Fig. 8 it is clear that below 0.2°K the BBP contribution is large but above 0.3°K the phonon process dominates.

After filling the cell with the appropriate solution we adjusted the focus and found the acoustic signal at the expected place. The amplitude was 15 dB smaller than expected; this may have been due to a matching layer problem. In order to check the result we allowed the temperature to drift up. The signal amplitude stayed constant until about 0.4 - 0.5K at which time it rapidly disappeared. The result was checked several times, drifting up and down in temperature. The total loss in our cell as predicted by Fig. 8 is shown in Fig. 9 and is consistent with our observations. From this result we can infer that the attenuation even in the solution is negligibly small at 1 GHz below 0.3°K. We are presently redesigning the lens to include a carbon matching layer and to extend the frequency of operation to 3 GHz where the wavelength will be 767 Å.

---

[14] J. Bardeen, G. Baym, and D. Pines, Phys. Rev. Lett. 17, 372 (1966).

[15] G. Baym and C. Ebner, Phys. Rev. 164, 235 (1967).

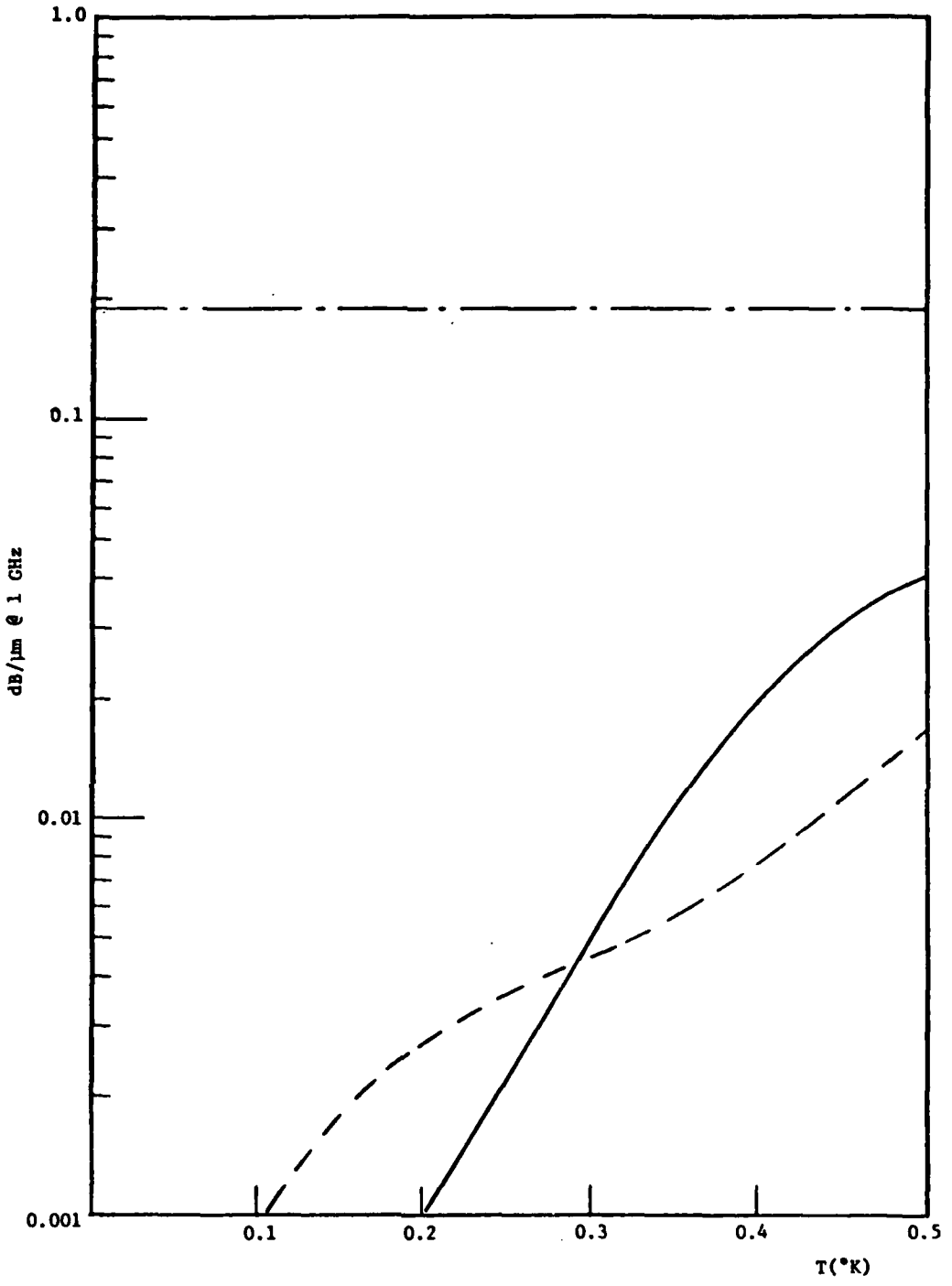

FIG. 8--Attenuation in liquid helium at low temperatures. Solid line is phonon contribution. Dashed line is ^{3}He quasiparticle contribution in a 2% ^{3}He-^{4}He solution. Upper line is 25°C water for comparison.

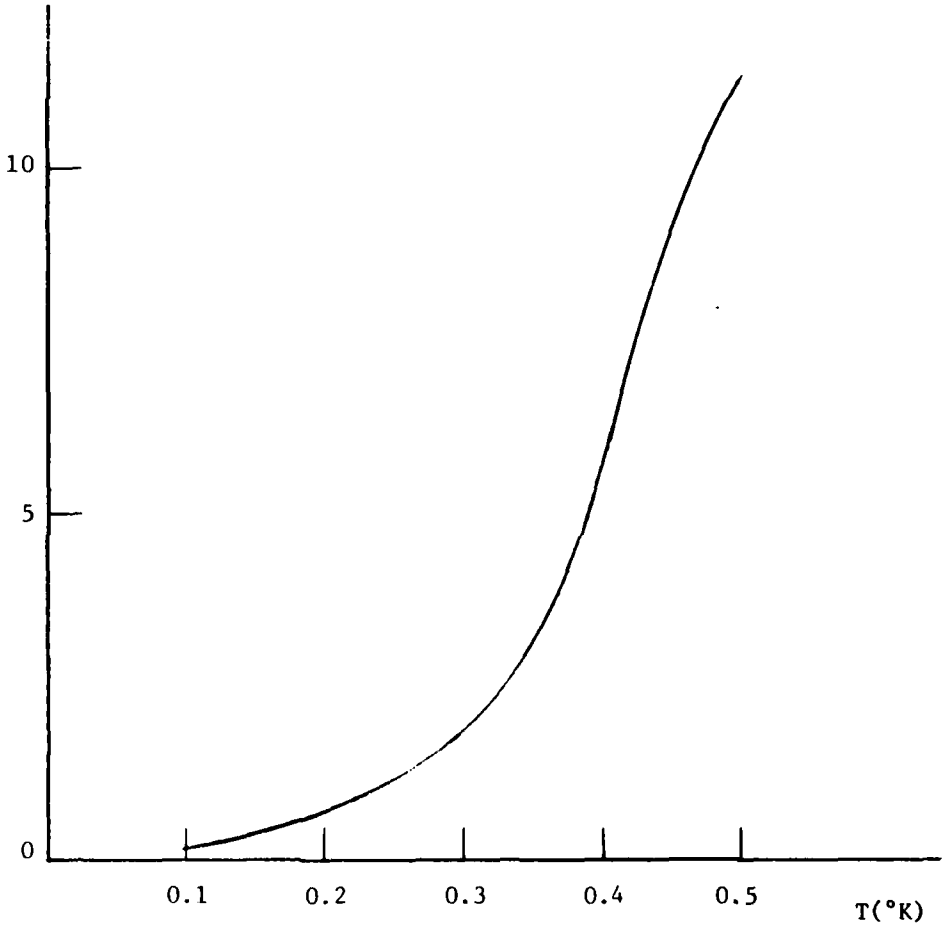

FIG. 9--Total attenuation in a 200 μm path in a 2% $^{3}He-^{4}He$ solution.

With increased signal-to-noise ratio we should be able to make a quantitative check on the BBP and phonon results. In addition, the theoretically interesting region near $\hbar\omega \approx kT$ will become accessible as we improve the thermal behavior of our probe.


DAT
FILM